Advances in ab initio studies of deformed nuclei and neutrinoless double-beta decay with renormalization group methods

Jiangming Yao (尧江明)

School of Physics and Astronomy, Sun Yat-sen University

Exploring nuclear physics across energy scales, April 27， 2024, Beijing

Outline

Probe new physics at the nuclear energy scale

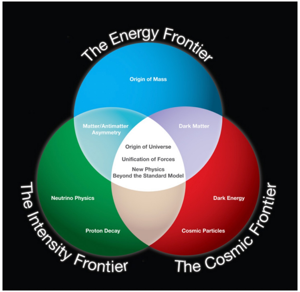

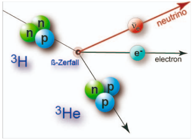

Single-beta decay

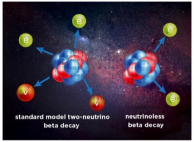

Neutrinoless double beta decay

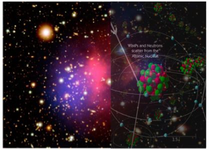

Dark matter direct detection

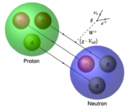

Superallowed Fermi transitions

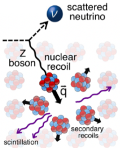

Neutrino scattering

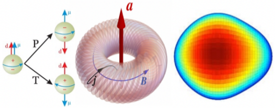

Symmetry-violating moments

- Frontiers in physics
- Testing fundamental symmetries and interactions.
- Low-energy probes
- Requiring accurate nuclear matrix elements (NMEs)

- The long-standing goal (tenet) in nuclear physics: *Do the same nuclear forces that explain free-space scattering experiments also explain the properties of finite nuclei and nuclear matter when applied in nuclear many-body theory?*
- Definition of ab initio theory in nuclear physics: vary with persons
  1. *We interpret the ab initio method as a systematically improvable approach employing Lagrangians, Hamiltonians, or energy density functionals derived from the Standard Model according to the principles of EFT.* A. Ekström et al., Front. Phys. 11, 1129094 (2023)
  2. *A true ab initio theory should define itself consistently and pass the test of the tenet with high precision.* R. Machleidt, Few-Body Systems 64, 77 (2023)
  3. In literature, *ab initio* has been popularly used to label theoretical analyses of nuclei based on "realistic" nucleon-nucleon, and three-nucleon potentials, with solutions to the nuclear many-body problem obtained either quasi-exactly or with controlled approximations.

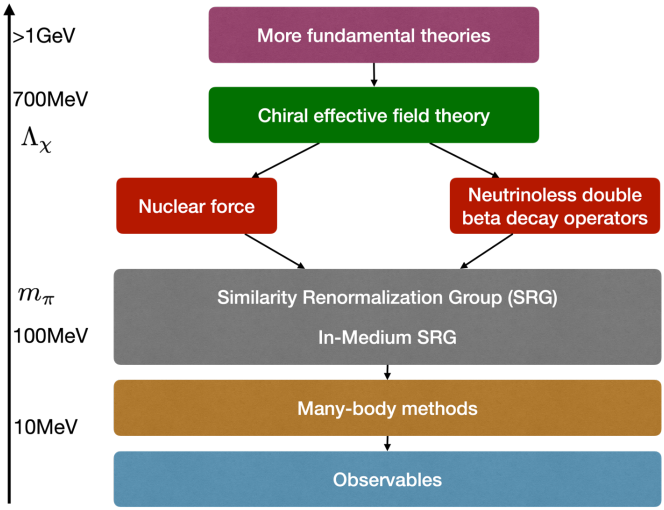

The basic idea of current efforts:

- Construct an EFT at the nuclear energy scale in terms of $N, \pi, (e, \nu)$ dofs.
- Match the EFT to more fundamental theories at higher-energy scales with the renormalization group (not work for nuclear force)
- Identify the relevant (chiral) symmetries, and write down all possible contributions according to a power counting rule, $(m_\pi, Q)/\Lambda_\chi$.

- Non-relativistic chiral 2N+3N interactions (Weinberg power counting and others)

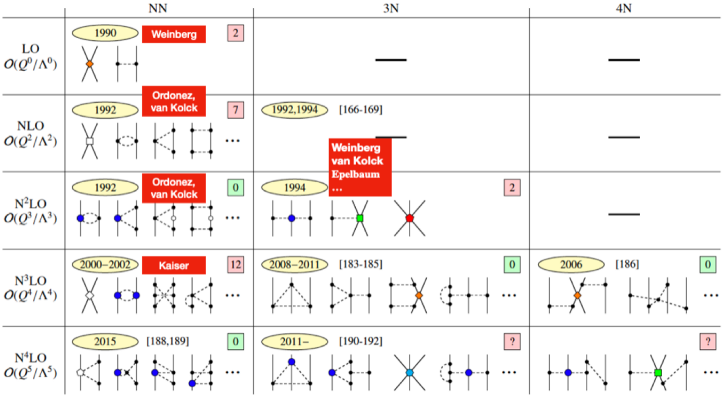

K. Hebeler, Phys. Rep. 890, 1 (2020)

- Relativistic chiral 2N interaction (up to N^{2}LO, different PC from the NR case)

J.-X. Lu et al., PRL128, 142002 (2022)

- Apply unitary transformations to decouple high and low-momentum states

$$H_s = U_s H U_s^\dagger \equiv T_{\rm rel} + V_s$$

from which one finds the flow equation

$$\frac{dH_s}{ds} = [\eta_s, H_s], \quad \eta_s = [T_{\rm rel}, H_s]$$

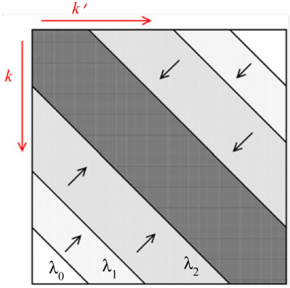

The flow parameter s is usually replaced with $\lambda = s^{-1/4}$ in units of fm^{-1} (a measure of the spread of off-diagonal strength).

Evolution of the potential

$$\frac{dV_s(k,k')}{ds} = -(k^2 - k'^2)V_s(k,k') + \frac{2}{\pi}\int_0^\infty q^2 dq (k^2 + k'^2 - 2q^2) V_s(k,q) V_s(q,k')$$

Preprocessing the nuclear potential with SRG

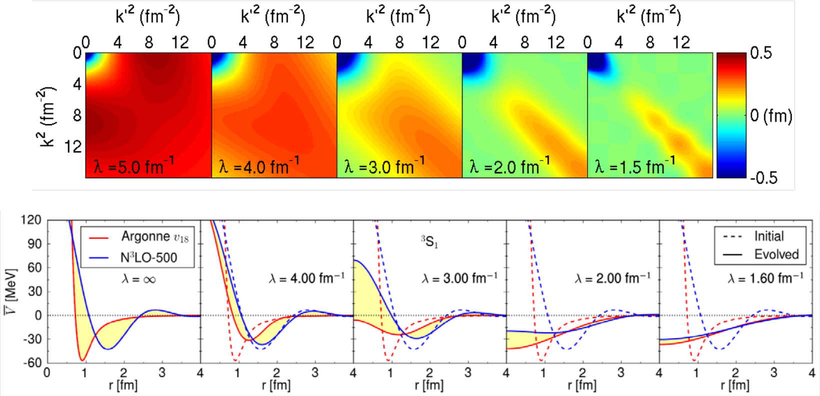

Local projection of AV18 and N^{3}LO(500 MeV) potentials $V(r)$.

- The hard core "disappears" in the SRG softened interactions

S. K. Bogner et al. PPNP (2010); Wendt et al. PRC (2012)

Preprocessing the Hamiltonian with IMSRG

- Apply unitary transformations to H in the configuration space

$$\hat{H}(s) = \hat{U}(s)\hat{H}_0\hat{U}^\dagger(s)$$

Flow equation

$$\frac{d\hat{H}(s)}{ds} = [\hat{\eta}(s), \hat{H}(s)]$$

- Generator $\eta(s)$: chosen either to decouple a given reference state from its excitations or to decouple the valence space from the excluded spaces.
- Not necessary to construct the whole H matrix in the config. space.

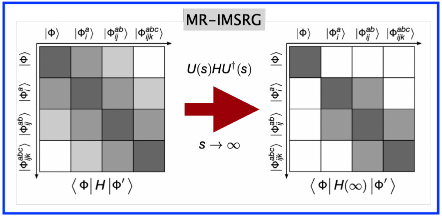

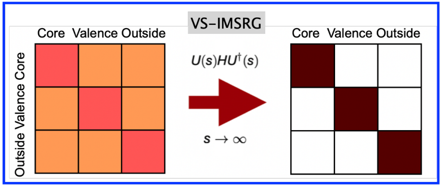

H. Hergert et al., Phys. Rep. 621, 165 (2016); S. R. Stroberg et al., Annu. Rev. Nucl. Part. Sci. 69, 307 (2019)

Prescription

- Pick a small model space (defined by emax) for the reference state
- Evolve the IMSRG flow in a large model space (defined by eMax)

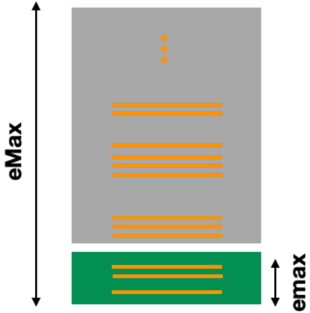

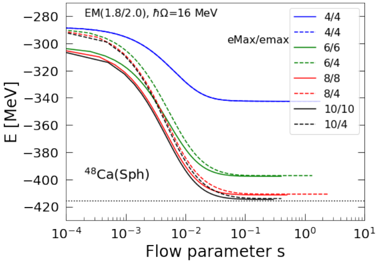

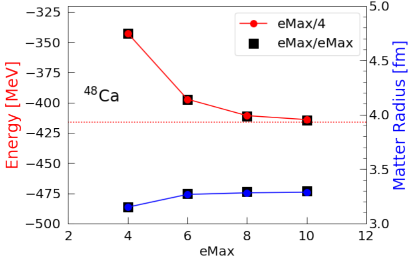

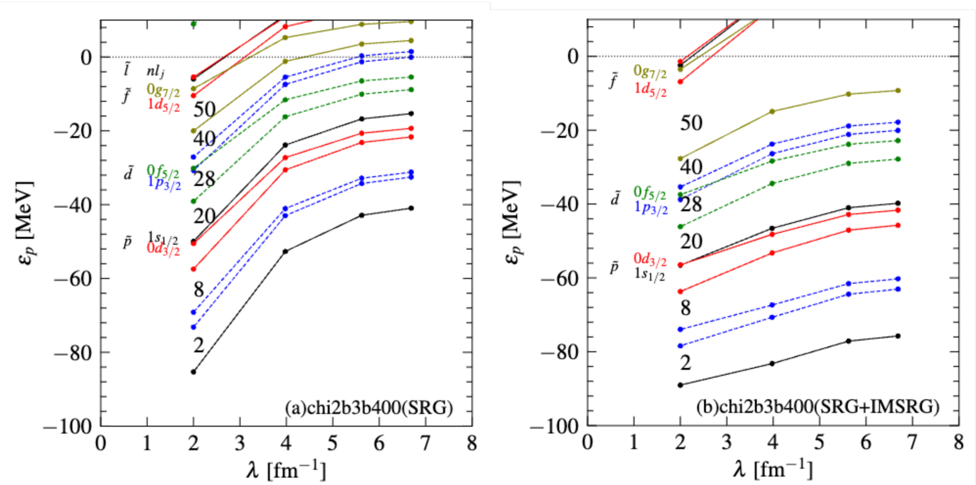

The large spin-orbit splittings and the approximate PSS emerge naturally in the ESPE spectra when the nuclear interaction evolves to a low-momentum scale.

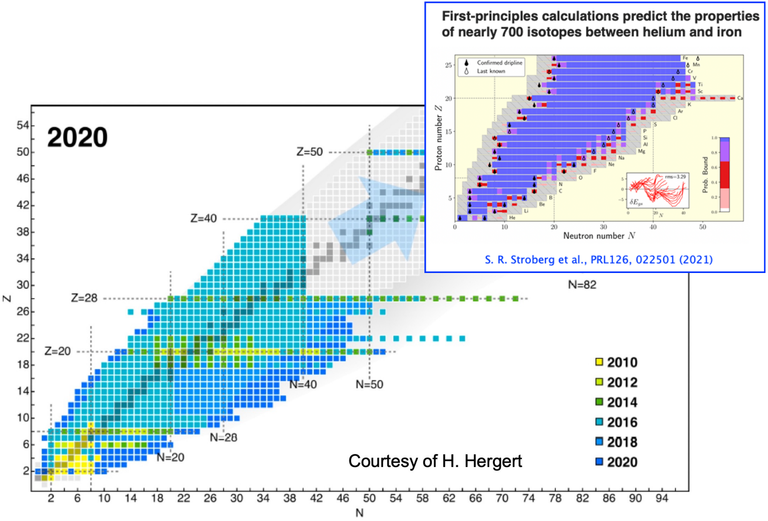
First-principles calculations predict the properties of nearly 700 isotopes between helium and iron
Confirmed dripline
Last known
Proton number Z
Neutron number N
Prob. Bound
S. R. Stroberg et al., PRL126, 022501 (2021)
2020
Z=50
Z=40
Z=28
Z=20
N=82
N=40
N=50
N=28
N=20
Courtesy of H. Hergert
2010
2012
2014
2016
2018
2020
Z
N

many-particle many-hole excitations

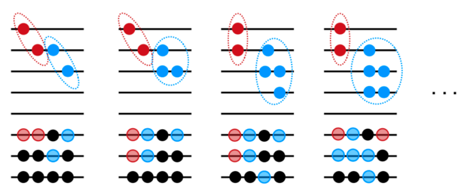

IMSRG(3)

- Computational scaling $O(N^9)$
- memory storage N^6

  computational chalenge!

IMSRG(A)

- From a simple HF reference state $|\Phi\rangle$ to exact ground state $|\Psi\rangle$

$$|\Psi\rangle = e^{\hat{\Omega}}|\Phi\rangle,$$

where many-body correlations are built into the correlation operator $\hat{\Omega}$,

$$\hat{\Omega} = \hat{\Omega}^{(1b)} + \hat{\Omega}^{(2b)} + \hat{\Omega}^{(3b)} + \cdots + \hat{\Omega}^{(Ab)}$$

determined from the IMSRG.

Multi-reference: Build collective correlations into the reference state (no core methods)

- From a correlated reference state $|\Phi\rangle$ to exact ground state $|\Psi\rangle$

$$|\Psi\rangle = e^{\hat{\Omega}}|\Phi_{\rm Cor}\rangle, \quad \hat{\Omega} = \hat{\Omega}^{(1b)} + \hat{\Omega}^{(2b)} + \cdots$$

  and the correlated reference state $|\Phi_{\rm Cor}\rangle$ can be chosen as a state with many-particle many-hole excitations relevant for nuclear collective excitations.
- IM-NCSM: reference state from NCSM calculation with a small $N_{\rm max}$

  E. Gebrerufael et al., PRL118, 152503 (2017)
- IM-GCM: reference state from PHFB/GCM calculation

  JMY et al., PRL124, 232501 (2020)

Cons: produce an effective interaction targeted for individual nucleus.

The Framework of IM-GCM

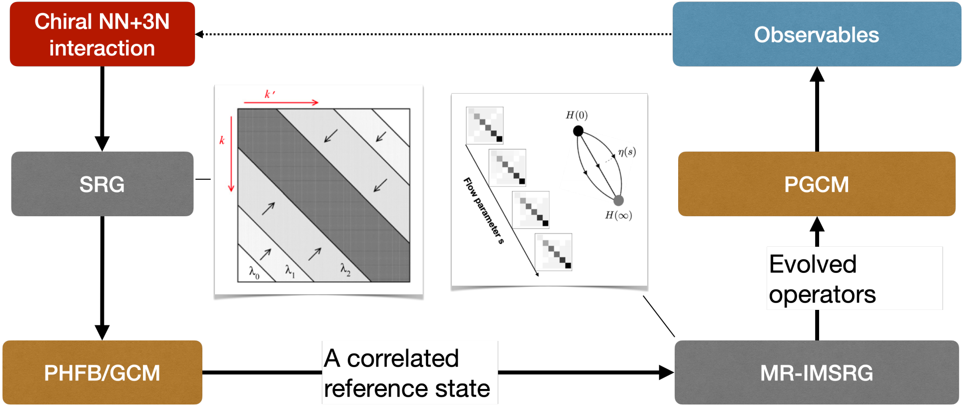

Application of IM-GCM to ^{48}Ca and ^{48}Ti

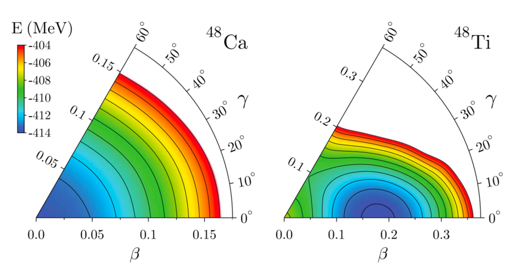

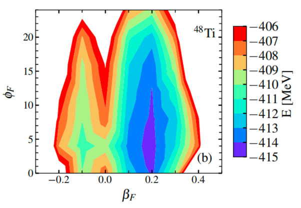

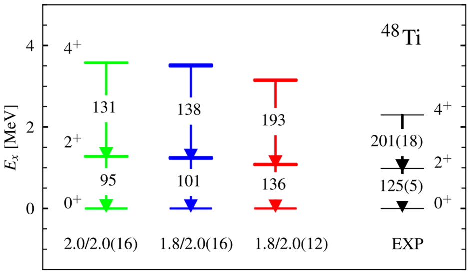

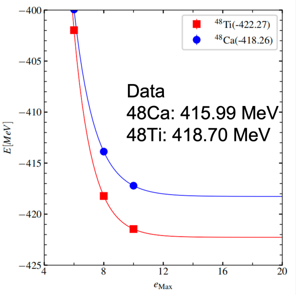

Application of IM-GCM to ^{76}Ge and ^{76}Se

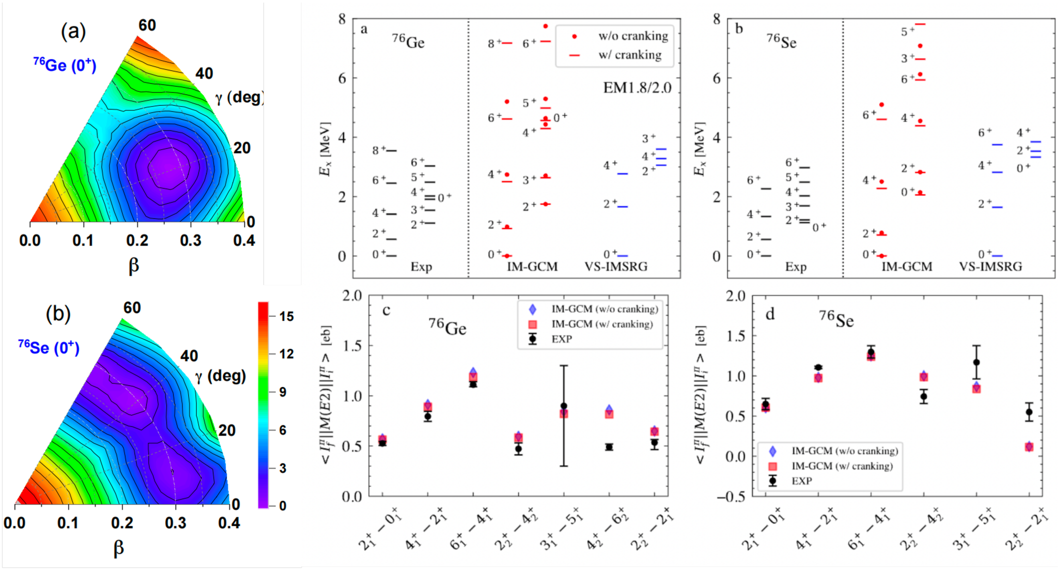

Application of IM-GCM to odd-mass nuclei

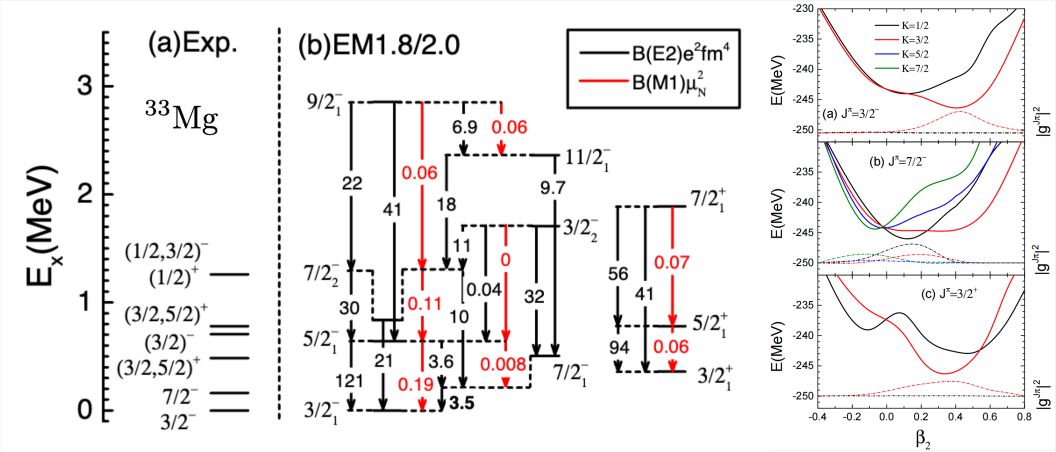

- Weak EM transitions from $7/2_1^-$ to ground state.
- $7/2_1^-$ is likely a shape isomer state.

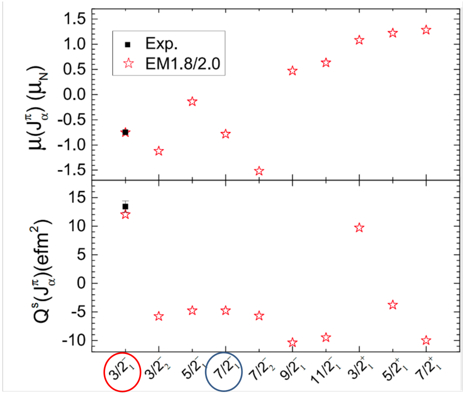

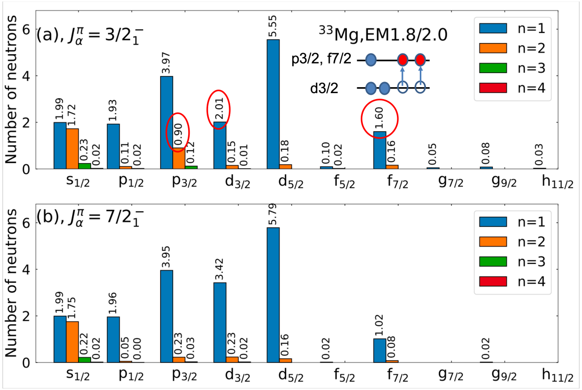

- Magnetic dipole moment and spectroscopic quadrupole moment of the ground state are reasonably reproduced, and the spin parity is $3/2^-$, which is a $2p$-$2h$ excitation compared to the $7/2^-_1$ state.

A special decay mode: $0\nu\beta\beta$ decay

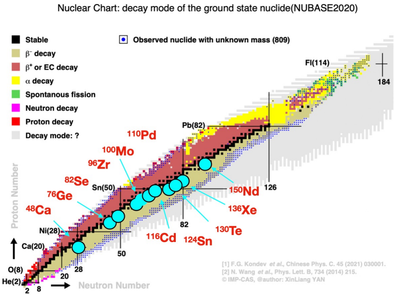

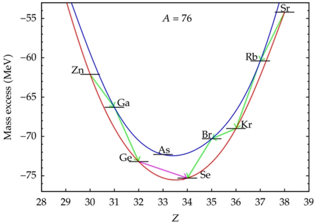

- The two modes of $\beta^-\beta^-$ decay:

$$(A, Z) \to (A, Z+2) + 2e^- + (2\bar{\nu}_e)$$

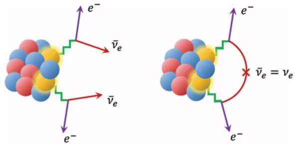

- Kinetic energy spectrum of electrons

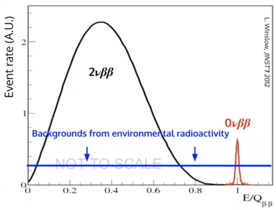

Status of measurements on $0\nu\beta\beta$ decay

Isotope	$G_{0\nu}$ $[10^{-14}\ \text{yr}^{-1}]$	$M^{0\nu}$ [min, max]	$T^{0\nu}_{1/2}$ [yr]	$\langle m_{\beta\beta}\rangle$ [meV]	Experiments References
^{48}Ca	2.48	[0.85, 2.94]	$> 5.8 \cdot 10^{22}$	[2841, 9828]	CANDLES: PRC78, 058501 (2008)
^{76}Ge	0.24	[2.38, 6.64]	$> 1.8 \cdot 10^{26}$	[73, 204]	GERDA: PRL125, 252502(2020)
^{82}Se	1.01	[2.72, 5.30]	$> 4.6 \cdot 10^{24}$	[277, 540]	CUPID-0: PRL129, 111801 (2023)
^{96}Zr	2.06	[2.86, 6.47]	$> 9.2 \cdot 10^{21}$	[3557, 8047]	NPA847, 168 (2010)
^{100}Mo	1.59	[3.84, 6.59]	$> 1.5 \cdot 10^{24}$	[310, 540]	CUPID-Mo: PRL126, 181802(2021)
^{116}Cd	0.48	[3.29, 5.52]	$> 2.2 \cdot 10^{23}$	[1766, 2963]	PRD 98, 092007 (2018)
^{130}Te	1.42	[1.37, 6.41]	$> 2.2 \cdot 10^{25}$	[88, 413]	CUORE: Nature 604, 53(2022)
^{136}Xe	1.46	[1.11, 4.77]	$> 2.3 \cdot 10^{26}$	[36, 156]	KamLAND-Zen: PRL130, 051801(2023)
^{150}Nd	6.30	[1.71, 5.60]	$> 2.0 \cdot 10^{22}$	[1593, 5219]	NEMO-3: PRD 94, 072003 (2016)

Note: $g_A = 1.27$, $G_{0\nu}$ is taken from J. Kotila and F. Iachello, Phys. Rev. C 85, 034316 (2012)

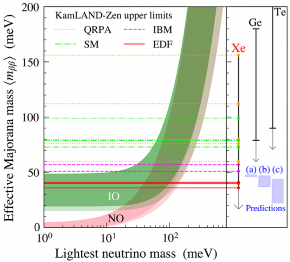

$$\langle m_{\beta\beta}\rangle = m_1 c_{12}^2 c_{13}^2 + m_2 c_{13}^2 s_{12}^2 e^{i\alpha_{21}} + m_3 s_{13}^2 e^{i(\alpha_{31}-2\delta)}$$

- The best lifetime sensitivity by KamLAND-Zen reaches the parameter space of IO case: $\langle m_{\beta\beta}\rangle \in [18, 50]$ meV.
- An uncertainty of a factor of about 3 or even more (originated from the $M^{0\nu}$) in the $\langle m_{\beta\beta}\rangle$.

Next-generation of experiments

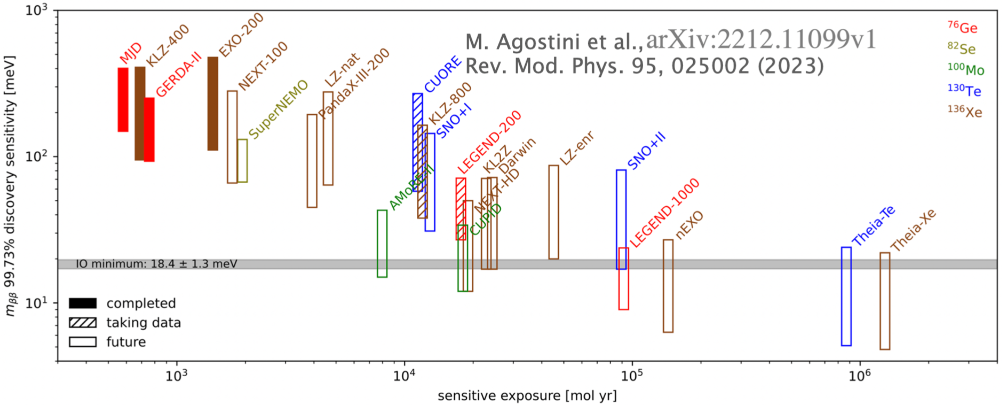

- Lifetime sensitivity of the ton-scale experiments: $> 10^{28}$yr.
- Whether or not the ton-scale experiments are able to cover the entire parameter space for the IO case depends strongly on the employed NME.

Comparison of nuclear models

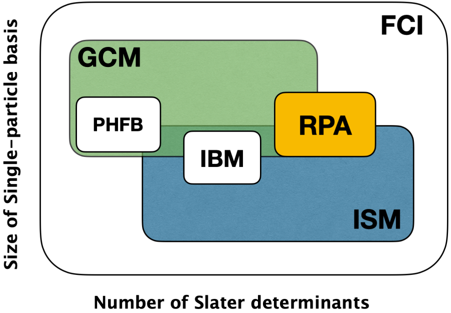

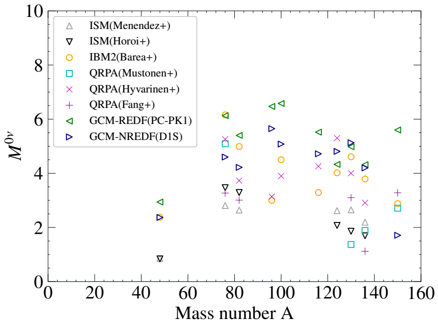

JMY, J. Meng, Y.F. Niu, P. Ring, PPNP 126, 103965 (2022)

- ISM predicts small NMEs, while IBM and EDF predict large NMEs. Discrepancy is about a factor of THREE or even larger.
- Statistical (fluctuation in input parameters) and systematical (model approximations) uncertainties are to be quantified.
- Efforts in resolving the discrepancy: very challenging!

Emulating GCM with the EC: the Lipkin model

- The Hamiltonian of the Lipkin model

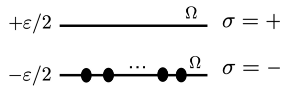

$$\hat{H} = \frac{\varepsilon}{2}\sum_{\sigma m}\sigma \hat{c}^{\dagger}_{\sigma m}\hat{c}_{\sigma m} - \frac{V}{2}\sum_{mm'\sigma}\hat{c}^{\dagger}_{\sigma m}\hat{c}^{\dagger}_{\sigma m'}\hat{c}_{-\sigma m'}\hat{c}_{-\sigma m}$$
$$= \varepsilon\hat{K}_0 - \frac{V}{2}(\hat{K}_+\hat{K}_+ + \hat{K}_-\hat{K}_-), \qquad \chi = \frac{V}{\varepsilon}(\Omega-1)$$

- GCM wave function

$$|\Psi^{\kappa}_{\rm GCM}(\chi)\rangle = \sum_{\mathbf{q}=1}^{N_{\rm q}} f^{\kappa}(\chi;\mathbf{q})\,|\Phi(\mathbf{q})\rangle$$

$$|\Phi(\alpha,\varphi)\rangle = \prod_{m=1}^{\Omega} a^{\dagger}_{0m}(\alpha,\varphi)|-\rangle$$

- EC+GCM wave function

$$|\Psi^{k}_{\rm EC}(\chi_{\odot})\rangle = \sum_{\kappa=1}^{k_{\rm max}\geq k}\sum_{t=1}^{N_t} g^{k}(\kappa,\chi_t)\,|\Psi^{\kappa}_{\rm GCM}(\chi_t)\rangle$$

Generalized eigenvalue equation

$$\sum_{\kappa'=1}^{k_{\rm max}}\sum_{t'=1}^{N_t}\left[\mathcal{H}^{\kappa\kappa'}_{tt'}(\chi_{\odot}) - E^{k}_{\chi_{\odot}}N^{\kappa\kappa'}_{tt'}\right]g^{k}(\kappa',\chi_{t'}) = 0,$$

QY Luo, X Zhang, LH Chen, JMY, arXiv:2404.08581

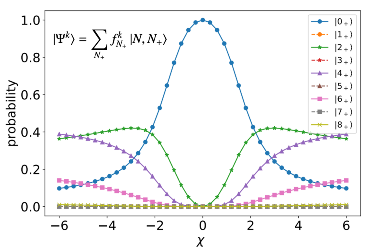

Diagonalization method

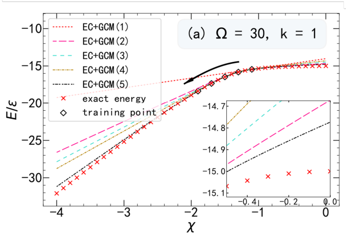

EC_1 +GCM

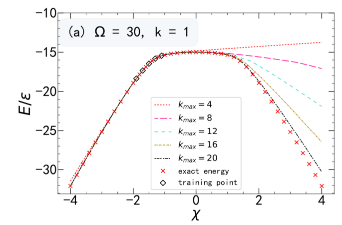

$\mathrm{EC}_{\rm kmax}$ +GCM

Sensitivity analysis with EC+MR-CDFT

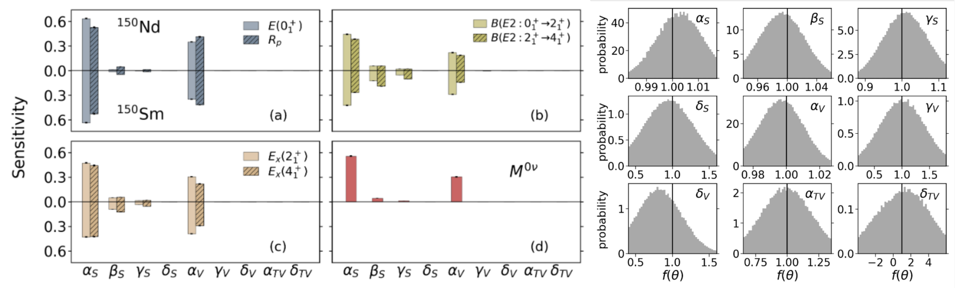

- 9 parameters $(\alpha_S, \beta_S, \gamma_S, \delta_S, \alpha_V, \gamma_V, \delta_V, \alpha_{TV}, \delta_{TV})$ in the relativistic EDF.
- 32 training Hamiltonians $H(c_i)$ and 32 test Hamiltonians $H(c_t)$
- Global sensitivity-analysis of $1,310,720$ emulations of MR-CDFT calculations (sampling EDFs around PC-PK1, corresponding $f(\theta) = 1$).
- Posterior distributions of input parameters by Bayesian analysis based on the $E_x(2_1^+)$.

X. Zhang, C.R. Ding, JMY, in preparation (2024)

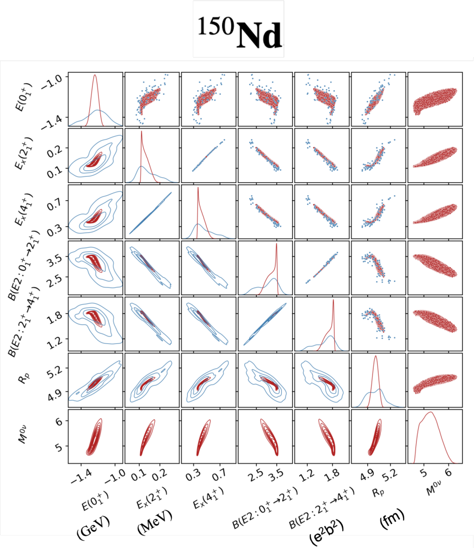

^{150}Nd
$E(0_1^+)$ (GeV)
$E_x(2_1^+)$ (MeV)
$E_x(4_1^+)$
$B(E2:0_1^+\to2_1^+)$
$B(E2:2_1^+\to4_1^+)$ (e^2b^2)
R_p (fm)
$M^{0\nu}$

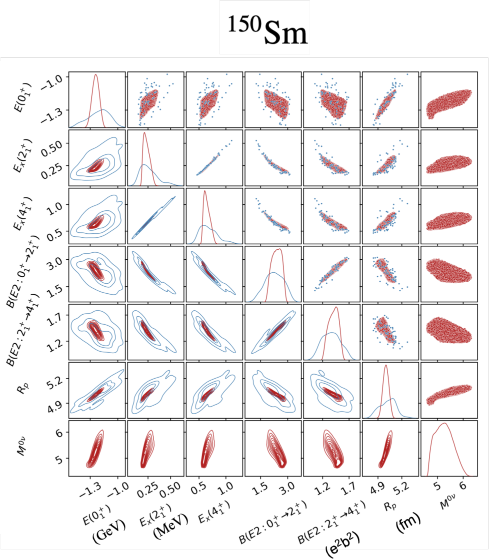

^{150}Sm
$E(0_1^+)$ (GeV)
$E_x(2_1^+)$ (MeV)
$E_x(4_1^+)$
$B(E2:0_1^+\to2_1^+)$
$B(E2:2_1^+\to4_1^+)$ (e^2b^2)
R_p (fm)
$M^{0\nu}$

Statistical uncertainty in MR-CDFT

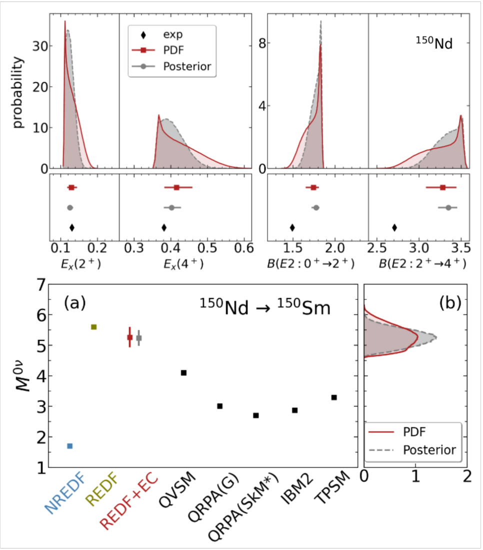

- The probability distribution function (pdf) is largely overlapping with the posterior distribution derived using the Bayesian method based on the correlation relation ($r = 0.93$) between the $M^{0\nu}$ and $E_x(2_1^+)$ of ^{150}Nd.
- The obtained $M^{0\nu} = 5.27 \pm 0.33$, slightly smaller than the previous value 5.60 [1].

[1] JMY, Song, Hagino, Ring, Meng, PRC91, 024316 (2015).

- At $E \sim$100 MeV: operators are expressed in terms of nucleons, pions, and leptons, arranged in the order $(Q, m_\pi/\Lambda_\chi)^\nu$,

$$\nu = 2A + 2L - 2 + \sum_i \left(\frac{n_f}{2} + d - 2 + n_e\right)_i$$

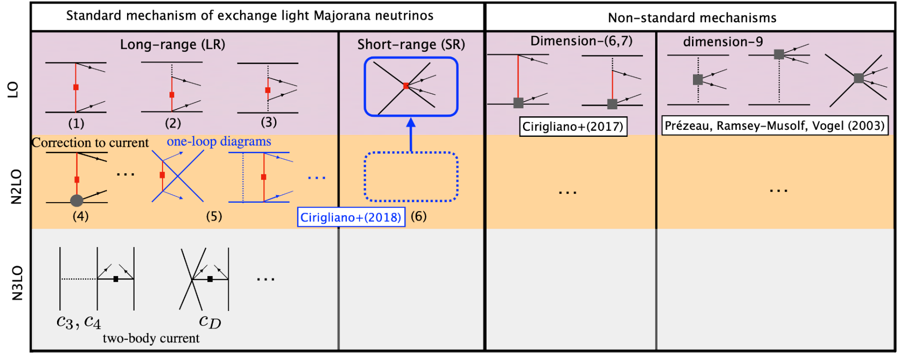

Ab initio methods for the lightest candidate ^{48}Ca

- Multi-reference in-medium generator coordinate method (IM-GCM)

  JMY et al., PRL124, 232501 (2020)

- IMSRG+ISM (VS-IMSRG)

  A. Belley et al., PRL126, 042502 (2021)

- Coupled-cluster with singlets, doublets, and partial triplets (CCSDT1) .

  S. Novario et al., PRL126, 182502 (2021)

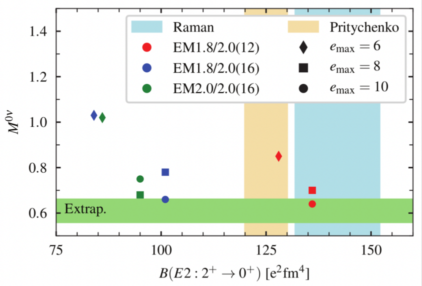

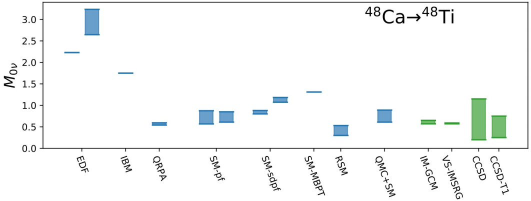

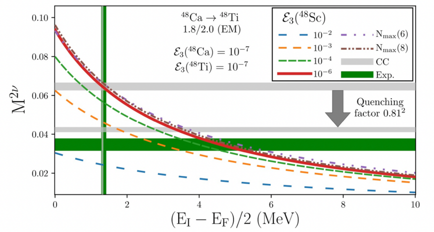

The missing piece in the LO transition operators

Featured in Physics | Editors' Suggestion | Open Access

New Leading Contribution to Neutrinoless Double-β Decay

Vincenzo Cirigliano, Wouter Dekens, Jordy de Vries, Michael L. Graesser, Emanuele Mereghetti, Saori Pastore, and Ubirajara van Kolck
Phys. Rev. Lett. **120**, 202001 – Published 16 May 2018

Physics See Synopsis: A Missing Piece in the Neutrinoless Beta-Dec

Nuclear force

Transition operator

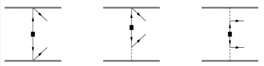

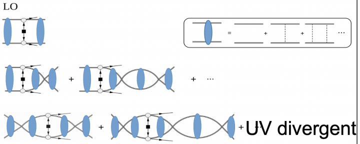

UV divergent

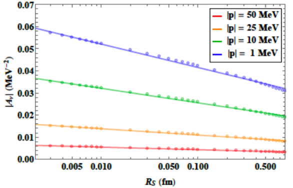

Lines fitted to $\mathcal{A}_\nu = a + b \ln R_S$

logarithmic dependence on R_S

Introducing a contact transition operator

$$V_{\nu,S} = -2 g_\nu^{NN} \tau^{(1)+} \tau^{(2)+}$$

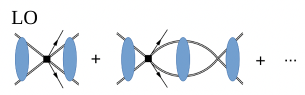

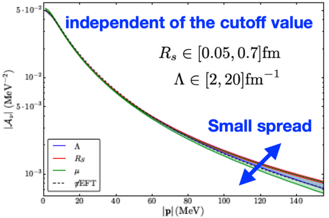

- The transition amplitude is regulator-dependent!
- Needs a counter term at LO in order to ensure renormalizability.

Toward Complete Leading-Order Predictions for Neutrinoless Double β Decay

Vincenzo Cirigliano, Wouter Dekens, Jordy de Vries, Martin Hoferichter, and Emar Mereghetti

Phys. Rev. Lett. **126**, 172002 (2021) – Published 30 April 2021

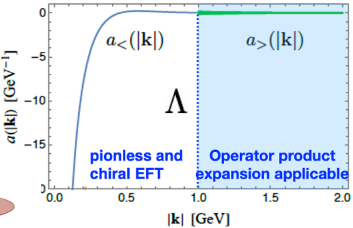

- **Cottingham formula** W.N. Cottingham, Ann. Phys. 25, 424 (1963)

$$\mathcal{A}_\nu \propto \int \frac{d^4k}{(2\pi)^4}\frac{g_{\mu\nu}}{k^2+i\epsilon}\int d^4x\, e^{ik\cdot x}\langle pp|T\{j^\mu_{\rm w}(x)j^\nu_{\rm w}(0)\}|nn\rangle$$

$$\mathcal{A}_\nu =$$

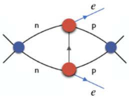

$$\propto \int \frac{d^4k}{(2\pi)^4}\frac{1}{k^2+i\epsilon}$$

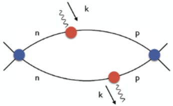

forward Compton amplitude

$$\mathcal{A}^{\rm full}_\nu = \int_0^\infty d|\mathbf{k}|\; a^{\rm full}(|\mathbf{k}|) = \mathcal{A}^< + \mathcal{A}^>\,,$$

$$\mathcal{A}^< = \int_0^\Lambda d|\mathbf{k}|\; a_<(|\mathbf{k}|)\,,$$

$$\mathcal{A}^> = \int_\Lambda^\infty d|\mathbf{k}|\; a_>(|\mathbf{k}|)\,,$$

- **Synthetic datum**

$$\mathcal{A}_\nu(|\mathbf{p}|,|\mathbf{p}'|)\times e^{-i(\delta_{^1S_0}(|\mathbf{p}|)+\delta_{^1S_0}(|\mathbf{p}'|))} = -\left(2.271 - 0.075\,\tilde{\mathcal{C}}_1(4\,M_\pi)\right)\times 10^{-2}\,\mathrm{MeV}^{-2}$$

$$\boxed{|\mathbf{p}| = 25\,\mathrm{MeV}\;(|\mathbf{p}'| = 30\,\mathrm{MeV})} \qquad = -1.95(5)_{\tilde{\mathcal{C}}_1}\times 10^{-2}\,\mathrm{MeV}^{-2}\,,$$

Uncertainty from the estimate of the **inelastic** contributions

The transition amplitude is observable and thus scheme independent.

A recent study in the relativistic chiral EFT shows that

- the $nn \to ppe^-e^-$ transition amplitude $\mathcal{A}_\nu$ is regulator-independent, thus no need to introduce the contact transition operator.
- The predicted $\mathcal{A}_\nu = 0.02085\mathrm{MeV}^{-2}$, about 10% larger than the value by Cirigliano (2021).
- The discrepancy could be attributed to the different power counting: the LO of relativistic chiral EFT contains partial N2LO contribution of non-relativstic EFT.

Y.L. Yang and P. W. Zhao, arXiv:2308.03356v1 (2023)

Bethe-Salpeter equation

$$T(\vec{p}\,',\vec{p}) = V(\vec{p}\,',\vec{p}) + \int \frac{d^3p''}{(2\pi)^3} V(\vec{p}\,',\vec{p}\,'') \frac{M_N^2}{E_{p''}} \frac{1}{p^2 - p''^2 + i\epsilon} T(\vec{p}\,'',\vec{p})$$

$$\boxed{E_{p''} \equiv \sqrt{M_N^2 + p''^2}.}$$

Lippmann-Schwinger equation

$$\widehat{T}(\vec{p}\,',\vec{p}) = \widehat{V}(\vec{p}\,',\vec{p}) + \int d^3p'' \widehat{V}(\vec{p}\,',\vec{p}\,'') \frac{M_N}{p^2 - p''^2 + i\epsilon} \widehat{T}(\vec{p}\,'',\vec{p})$$

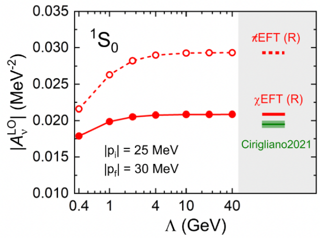

Within the non-relativistic chiral EFT,

- The LEC g_ν^{NN} consistent with the employed chiral interaction (EM1.8/2.0) is determined based on the synthetic data.
- The contact term turns out to enhance (instead of qunech) the NME for ^{48}Ca by 43(7)%, thus the half-life $T_{1/2}^{0\nu\beta\beta}$ is only half of the previously expected value.
- The uncertainty (7%) is due to the synthetic data which can be reduced by using an accurate value of the LEC (g_ν^{NN}).

R. Wirth, JMY, H. Hergert, PRL127, 242502 (2021)

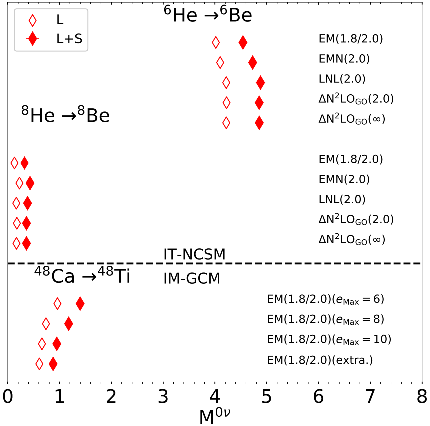

VS-IMSRG method for $0\nu\beta\beta$ decay of heavier candidates

With both the long- and short-range transition operators, the VS-IMSRG method is applied to study the NMEs of heavier candidates:

- For ^{130}Te, $M^{0\nu}_{L+S} \in [1.52, 2.40]$
- For ^{136}Xe, $M^{0\nu}_{L+S} \in [1.08, 1.90]$

The uncertainty is composed of different sources: nuclear interaction, reference-state, basis extrapolation, closure approximation, and the LEC for the short-range transition operators.

The values are generally smaller than those from phenomenological nuclear models.

A. Belley et al, arXiv:2307.15156 (2023)

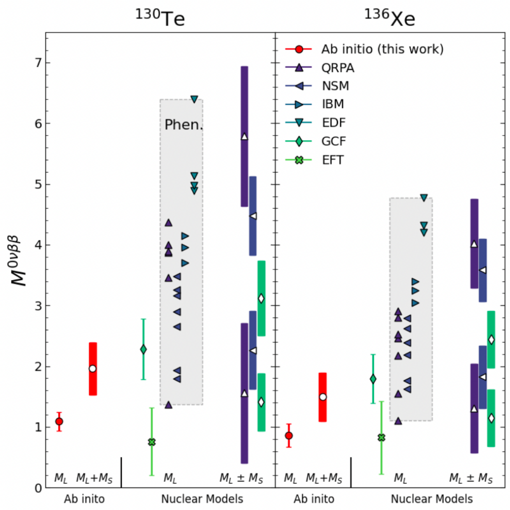

A more comprehensive quantification analysis

different nuclear many-body solvers, convergence of NMEs with chiral expansion orders, etc.

Convergence w.r.t. the chiral expansion order for nuclear forces

中山大學 SUN YAT-SEN UNIVERSITY

$2n \rightarrow 2p + 2e^-$

$^{48}\mathrm{Ca} \rightarrow ^{48}\mathrm{Ti} + 2e^-$

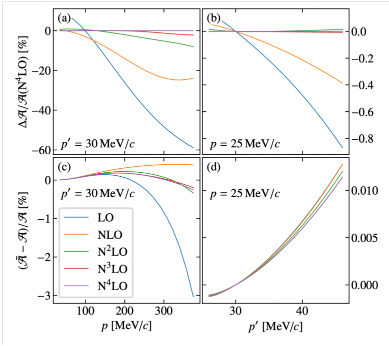

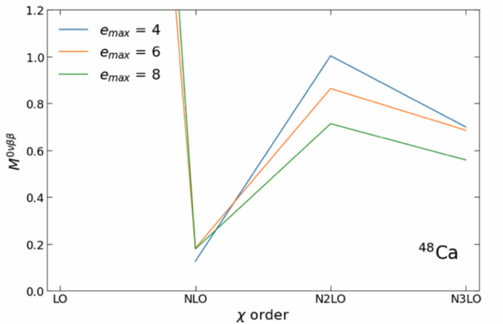

- The $\mathcal{A}_\nu(2n \rightarrow 2p + 2e^-)$ converges quickly w.r.t. the chiral expansion order of nuclear interactions. Negligible contribution beyond NLO, particular true for low momentum cases. R. Wirth, JMY, H. Hergert, PRL127, 242502 (2021)
- Convergence is slightly slower in candidate nucleus ^{48}Ca.

中山大學 SUN YAT-SEN UNIVERSITY

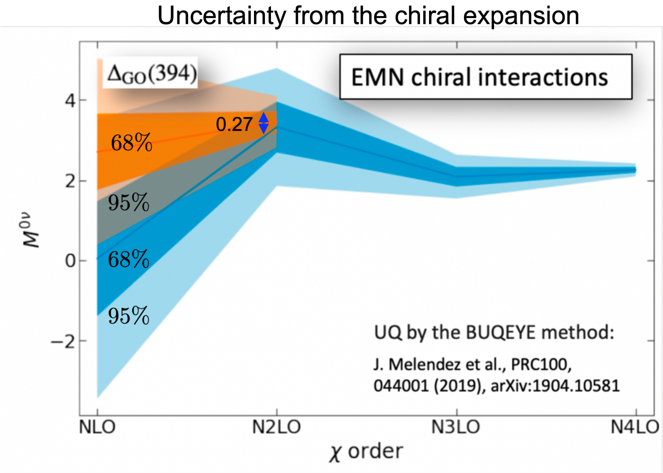

A. Belley, JMY et al, PRL, in press (2024)

- NME at the LO

$$\tilde{M}^{0\nu}_{\rm LO} = \tilde{M}^{0\nu}_{\rm LO,LR} + M^{0\nu}_{\rm LO,SR}.$$

$$\boxed{\tilde{M}^{0\nu}_{\rm LO,LR} = M^{0\nu}_{\rm LO,LR}(1,2,3) + M^{0\nu}_{\rm N2LO,LR}(4).}$$

- The NME (~0.08) at the N2LO is less than 5% of that at the LO.
- The uncertainty in the SR transition operator is about 0.13.
- The use of closure approximation: ~10% error.

Power counting

$$\nu = 2A + 2L - 2 + \sum_i \left(\frac{n_f}{2} + d - 2 + n_e\right)$$

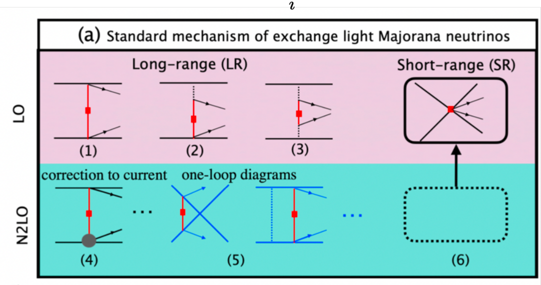

$e_{\rm Max}$	$M^{0\nu}_{\rm LO,LR}(1,2,3)$	$M^{0\nu}_{\rm LO,SR}$	$\tilde{M}^{0\nu}_{\rm LO,LR}$	$\tilde{M}^{0\nu}_{\rm LO}$	$M^{0\nu}_{\rm N2LO}(5)$
6	3.325	[0.872,1.152]	3.170	[4.04, 4.32]	0.196
8	2.092	[0.533,0.704]	2.020	[2.55, 2.72]	0.115
10	1.813	[0.437,0.577]	1.744	[2.18, 2.32]	0.090
extrap.	1.732	[0.399, 0.526]	1.670	[2.07, 2.20]	0.079

A. Belley, JMY et al, PRL, in press (2024)

Quantification of statistic uncertainty in the NME of ^{76}Ge

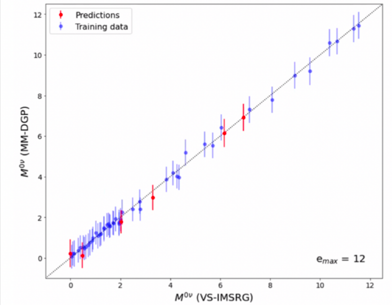

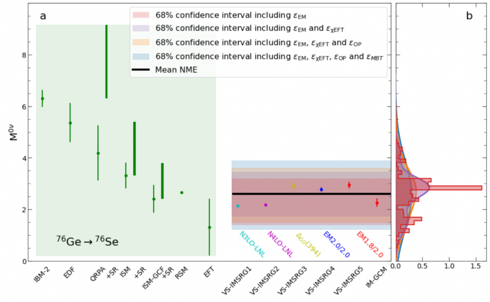

- Emulator, 8188 samples of chiral interactions, phase shift, $M^{0\nu} = 3.44^{+1.33}_{-1.56}$.
- Including the g.s. energies of $A = 2, 3, 4, 16$ and phase shift: $M^{0\nu} = 2.60^{+1.28}_{-1.36}$, which gives the effective neutrino mass $\langle m_{\beta\beta} \rangle = 187^{+205}_{-62}$ meV.
- The next-generation ton-scale Germanium experiment ($\sim 1.3 \times 10^{28}$ yr): $\langle m_{\beta\beta} \rangle = 22^{+24}_{-7}$ meV, covering almost the entire range of IO hierarchy.

A. Belley, JMY et al, PRL, in press (2024)

Summary and perspective

- Remarkable advances have been achieved in ab initio studies of nuclear structure and decays. However, the low-lying states of medium mass deformed nuclei are still challenging for most ab initio methods.
- The IM-GCM, a combination of IMSRG and GCM, stands out as a promising approach for the low-lying states of nuclei with complicated shapes. It has been successfully applied to describe the low-lying states of $0\nu\beta\beta$ decay candidate nuclei ^{48}Ti, ^{76}Ge, ^{76}Se, and odd-mass nuclei ^{33}Mg.
- The NMEs for the $0\nu\beta\beta$ decay in ^{48}Ca and ^{76}Ge have been determined with uncertainty quantification. Convergence w.r.t. the chiral expansion order turns out to be rather rapid.

Next

- Schiff moments of odd-mass nuclei with octupole correlations, ^{225}Ra.
- The NMEs of heavier candidates ^{82}Se, ^{100}Mo, ^{130}Te, ^{136}Xe, with reduced uncertainty.

Acknowledgements

SUN YAT-SEN UNIVERSITY

Collaborators

- SYSU
  C.R. Ding, Q.Y. Luo, C.F. Jiao, C.C. Wang, G. Li, X. Zhang, E.F. Zhou
- PKU
  Lingshuang Song, Jie Meng, Peter Ring
- LZU: Yifei Niu
- CAEP: Bingnan Lv
- SWU: Longjun Wang
- MSU: Scott Bogner, Heiko Hergert, Roland Wirth
- UNC: Jonathan Engel, A. M. Romero
- TRIUMF: Antonie Belly, Jason Holt
- TU Darmstadt: Takayuki Miyagi
- Notre-Dame U: Ragnar Stroberg
- UAM: Benjamin Bally, Tomas Rodriguez

This work is supported in part by the National Natural Science Foundation of China (Grant Nos. 12141501 and 12275369), the Guangdong Basic and Applied Basic Research Foundation (2023A1515010936).

Thank you for your attention!

Test of the EC+MR-CDFT calculations

TABLE I. The rms deviations of the observables $E(0_1^+)$ (MeV), $E_x(2_1^+)$ (MeV), $B(E2: 0_1^+ \to 2_1^+)$ (e^2b^2) and R_p (fm) between the three types of emulators and the GCM calculations on the 32 testing points for ^{150}Nd and ^{150}Sm.

^{150}Nd	$\sigma[E(0_1^+)]$	$\sigma[E_x(2_1^+)]$	$\sigma[B(E2)]$	$\sigma[R_p]$
GCM(c_0)	5.9522	0.052	0.517	0.113
GCM(c_i^T)	0.2728	0.006	0.100	0.007
EC+GCM	0.2720	0.007	0.123	0.008
^{150}Sm				
GCM(c_0)	6.1291	0.081	0.505	0.106
GCM(c_i^T)	0.2875	0.186	0.154	0.093
EC+GCM	0.2717	0.040	0.212	0.007

Quantification of statistic uncertainty in the NME of ^{76}Ge

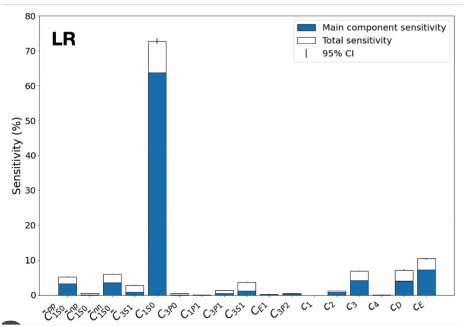

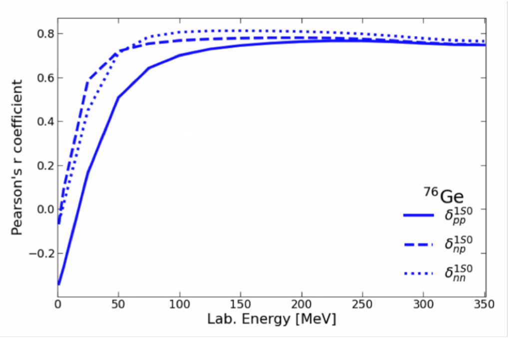

- The long-range part of the NME is sensitive to the LEC $C_{^1S_0}$.
- The phase shift of the $^1S_0$ channel is linearly correlated to the NME.
- The neutron-proton phase-shift δ_{np}^{1S0} at 50 MeV is used to weight the samples.

Isotope	$G_{0\nu}$ $[10^{-14}\ \mathrm{yr}^{-1}]$	$M^{0\nu}(\chi\mathrm{EFT})$ [min, max]	$T^{0\nu}_{1/2}$ [yr]	$\langle m_{\beta\beta}\rangle$ [meV]	Worldwide Exps current best limits	Inside China
76Ge	0.24	$2.60^{+1.27}_{-1.36}$	$> 1.8 \cdot 10^{26}$	187^{+205}_{-62}	GERDA: PRL125, 252502(2020)	CDEX
82Se	1.01		$> 4.6 \cdot 10^{24}$	.	CUPID-0: PRL129, 111801 (2023)	NvDEx
^{100}Mo	1.59		$> 1.5 \cdot 10^{24}$		CUPID-Mo: PRL126, 181802(2021)	CPUID-China
^{130}Te	1.42	[1.52, 2.40]	$> 2.2 \cdot 10^{25}$	[236, 373]	CUORE: Nature 604, 53(2022)	JUNO
^{136}Xe	1.46	[1.08, 1.90]	$> 2.3 \cdot 10^{26}$	[91, 160]	KamLAND-Zen: PRL130, 051801(2023)	PANDAX

Extension of the above uncertainty quantification to heavier candidates: ^{82}Se, ^{100}Mo and ^{130}Te, ^{136}Xe.

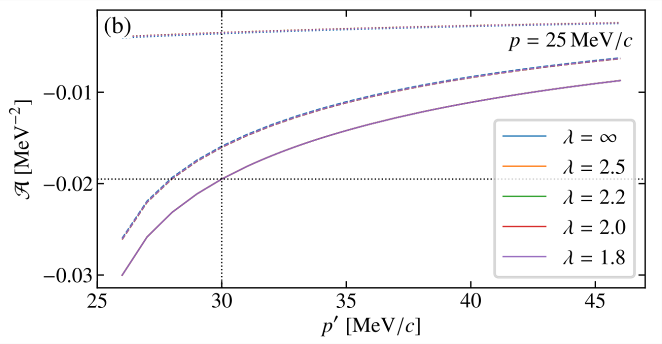

Figure: Momentum dependence of the short- and LO long-range parts, as well as the total amplitude for the EM potential at different SRG scales λ. Shown are the scaled short-range part $-2g_\nu^{NN}\mathcal{A}_S$ (dotted lines), the long-range part $\mathcal{A}_L$ (dashed lines), and the total amplitude $\mathcal{A}_L - 2g_\nu^{NN}\mathcal{A}_S$ (solid lines).

R. Wirth, JMY, H. Hergert, PRL127, 242502 (2021)

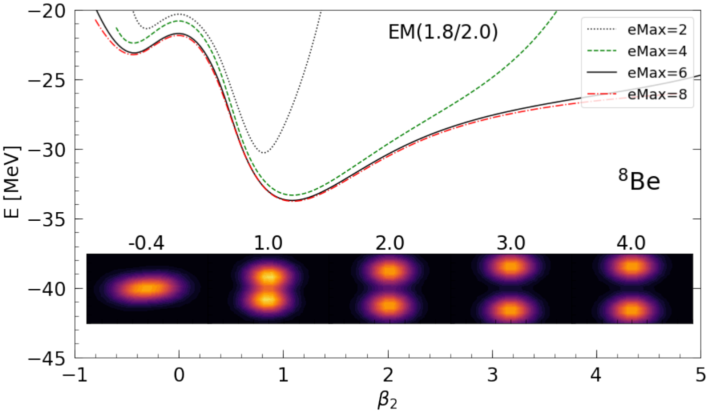

The SRG softened 2N chiral interaction from Entem & Machleidt with 3NF.

Two-alpha cluster structure in ^{8}Be

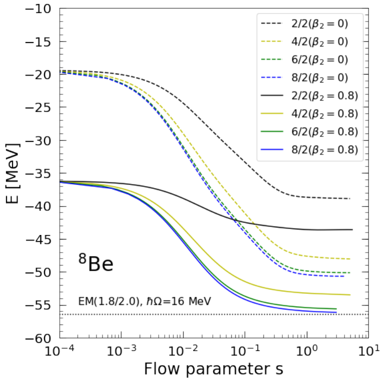

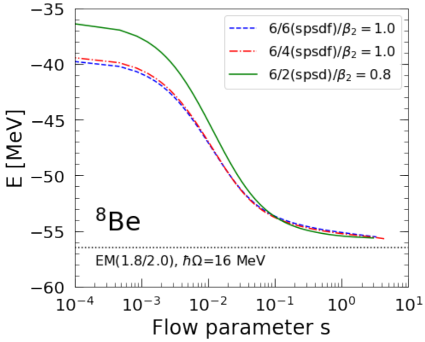

- Starting from the spherical or two-α cluster state, the IMSRG(2) is converged to different solution.
- Starting from the deformed states in different model space, the IMSRG(2) is converged to the same solution.

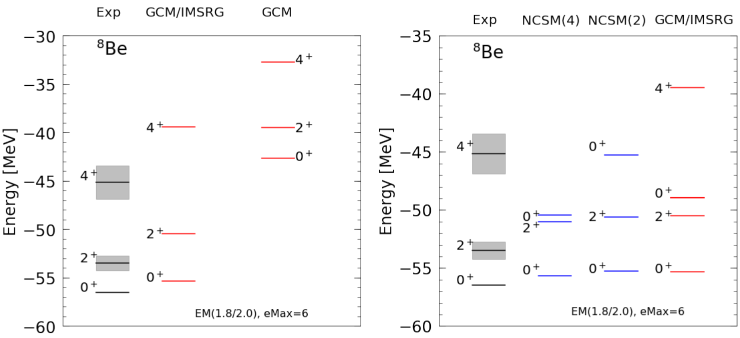

E2 transition (reference state $\beta_2 = 0.8$)

- $B(E2: 2_1^+ \to 0_1^+) = 5.77 e^2 \mathrm{fm}^4$, $R_m = 2.27$ fm (bare operator)
- $B(E2: 2_1^+ \to 0_1^+) = 8.76 e^2 \mathrm{fm}^4$, $R_m = 2.54$ fm (evolved operator)

SUN YAT-SEN UNIVERSITY

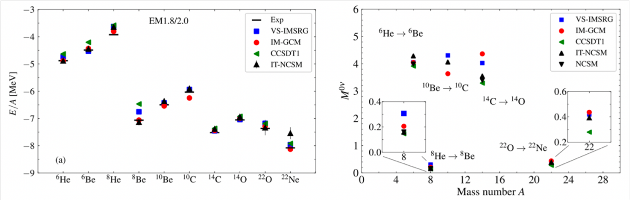

IM-GCM (EM1.8/2.0)

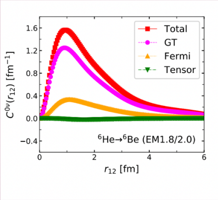

S. Pastore et al (2018)

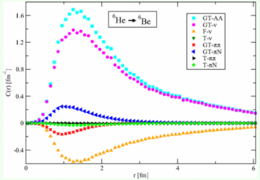

Note: A factor of $-g_A^2$ has been multiplied into the Fermi part.

JMY et al., PRC103, 014315 (2021)

- IT-NCSM and NCSM are quasi-exact methods, but limited to light nuclei.
- VS-IMSRG, IM-GCM, and CCSDT1 with some kinds of truncations can be applied to heavier candidate nuclei.
- Using different ab initio methods but the same input to estimate the truncation errors of the many-body methods.

Pairing fluctuation effect in MR-CDFT

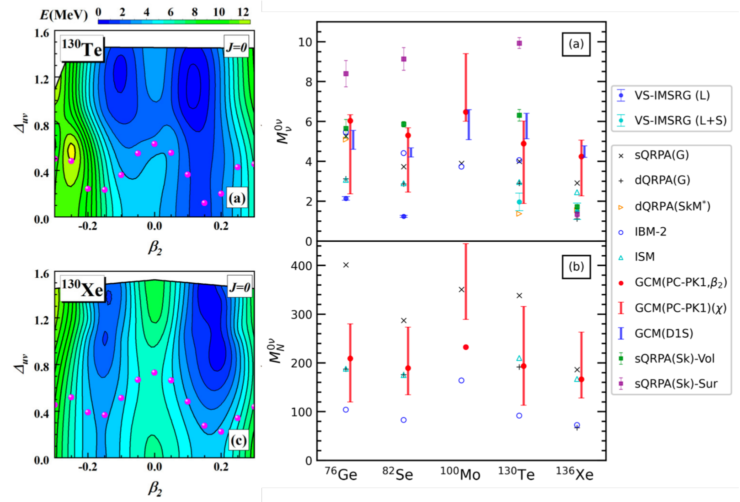

Ding, Zhang, JMY, Ring, Meng, PRC108, 054304 (2023)

Non-standard mechanism and constraints on LNV operators

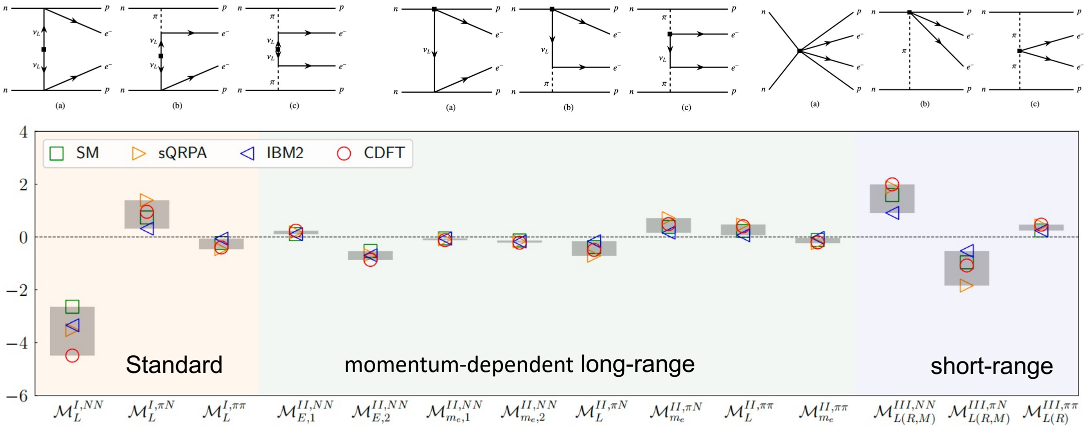

C.R. Ding, G. Li, JMY, arXiv:2403.17722v1 (2024)

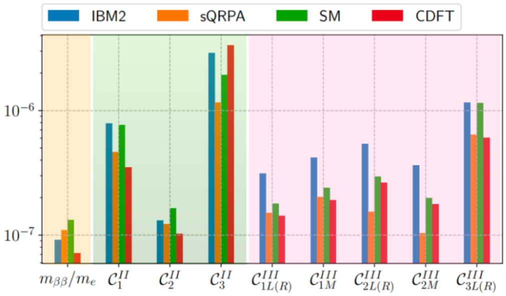

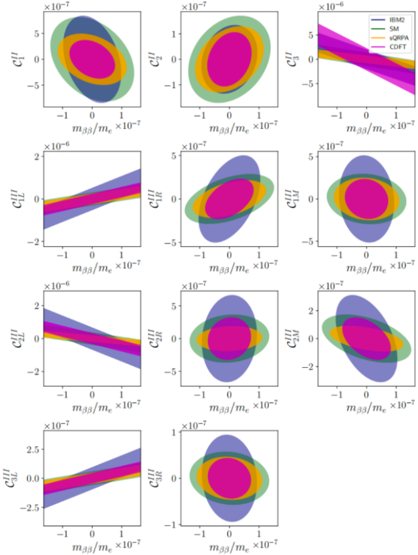

C.R. Ding, G. Li, JMY, arXiv:2403.17722v1 (2024)

The "magic" interaction EM1.8/2.0: The NN (N^3LO: D.R. Entem, R. Machleidt, PRC68 041001 (2003)) and local 3N interactions (N^2LO: K. Hebeler et al., PRC**83**, 031301(R) (2011)).

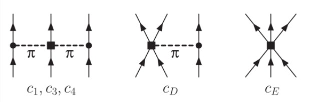

The LECs of the 3N are fitted on top of the SRG evolved NN interaction.

TABLE I. Results for the c_D and c_E couplings fit to $E_{^3\mathrm{H}} = -8.482$ MeV and to the point charge radius $r_{^4\mathrm{He}} = 1.464$ fm (based on Ref. [26]) for the NN/3N cutoffs and different EM/EGM/PWA c_i values used. For $V_{\mathrm{low}\,k}$ (SRG) interactions, the 3NF fits lead to $E_{^4\mathrm{He}} = -28.22\ldots-28.45$ MeV ($-28.53\ldots-28.71$ MeV).

	$V_{\mathrm{low}\,k}$		SRG	
Λ or $\lambda/\Lambda_{\mathrm{3NF}}$ (fm)	c_D	c_E	c_D	c_E
1.8/2.0 (EM c_i's)	+1.621	−0.143	+1.264	−0.120
2.0/2.0 (EM c_i's)	+1.705	−0.109	+1.271	−0.131
2.0/2.5 (EM c_i's)	+0.230	−0.538	−0.292	−0.592
2.2/2.0 (EM c_i's)	+1.575	−0.102	+1.214	−0.137
2.8/2.0 (EM c_i's)	+1.463	−0.029	+1.278	−0.078
2.0/2.0 (EGM c_i's)	−4.381	−1.126	−4.828	−1.152
2.0/2.0 (PWA c_i's)	−2.632	−0.677	−3.007	−0.686

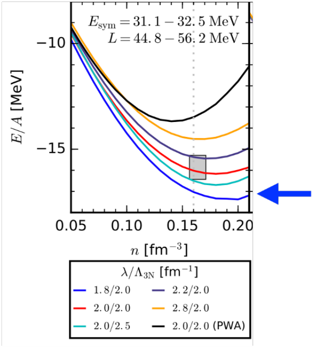

C. Drischler et al., PRL122, 042501 (2019)

The saturation properties are not well reproduced.

EFT: a model-independent analysis of operators at different energy scales

Cirigliano et al., JHEP (2018)

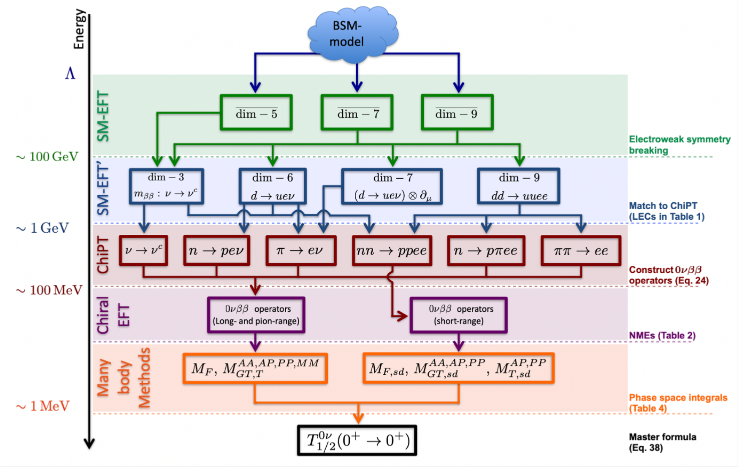

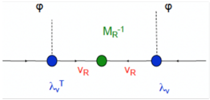

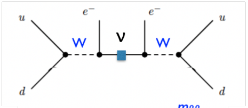

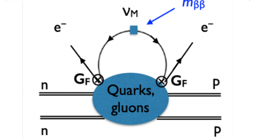

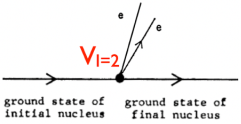

Temporary page!

LaTeX was unable to guess the total number of pages correctly. As there was some unprocessed data that should have been added to the final page this extra page has been added to receive it.

If you rerun the document (without altering it) this surplus page will go away, becau
LaTeX now knows how many pages to expect for this document.